Progress in Fractional Differentiation and Applications
An International Journal

http://dx.doi.org/10.18576/pfda/090213

On a Fractional Variable-Order Model of MERS-CoV

Mohamed Khalil[1,*], *Anas Arafa*[2] *and Amaal Sayed*[3]

[1] Department of Mathematics, Faculty of Engineering, October University for Modern Sciences and Arts (MSA), Giza, Egypt
[2] Department of Mathematics, College of Science and Arts, Qassim University, Al-Mithnab, Saudi Arabia
[3] Department of Basic Science, Faculty of Engineering, May University in Cairo (MUC), Cairo, Egypt

Received: 2 Sep. 2022, Revised: 18 Oct. 2022, Accepted: 20 Nov. 2022
Published online: 1 Apr. 2023

Abstract: In this paper, a non-integer variable-order epidemiological model is presented to study the human-to-human transmission of Middle East respiratory syndrome coronavirus (MERS-CoV) pandemic in two areas. In the presented SISI model, the human population is divided into two compartments; susceptible and infectious compartments. The impact of the memory which changes with time in the sense of Caputo's derivative of fractional variable-order is studied through the numerical solutions of the proposed model. The numerical solutions are obtained via predictor corrector method. Moreover, the equilibrium points and stability of the model are illustrated.

Keywords: Mathematical modeling of MERS-CoV, fractional variable-order epidemiological models, predictor corrector method.

1 Introduction

Infectious diseases have become one of the most serious global threats to human societies [1]. The prevalence of epidemics and pandemics shaped dramatically the human history. Through history, global pandemics including the Black Death, Cholera and the Spanish flu of 1918 affected human civilizations and killed millions of people [2]. Recently, Pandemics like SARS, bird flu (H5N1), swine flu (H1N1), Ebola, Zika and Covid-19 caused millions of deaths during the last few decades [3]. Moreover, endemic diseases like HIV, AIDS, TB and malaria are potentially deadly diseases that currently kill millions of people each year in several countries [4,5,6]. One of such infectious diseases is the Middle East respiratory syndrome coronavirus (MERS-CoV). It is a viral respiratory infectious disease which struck human societies [7]. In 2012, the first cases were discovered in the Middle East (in Saudi Arabia) and then it spread dramatically to other countries [8]. The virus mostly spread directly from human to human through close contact. It causes severe illness with a high threat of mortality. The economic impact of MERS-CoV outbreak was devastating through several sectors like tourism, international trade, international supply chains, agricultural, and services sectors [9].
Mathematical models of infectious diseases are very essential to give a detailed description of the prevalence of infectious diseases within a population [10,11]. Furthermore, such models are significant tools to figure out the crucial aspects of epidemics and to understand the dynamics of emerging infectious diseases. On the other hand, decision makers can use mathematical models to gather information about the behaviour of epidemics and pandemics in order to apply strategic plans to face the infectious diseases threat and to control infectious diseases. Fractional order models are valuable tools to describe epidemiological dynamical systems [12-20].
Such models represent better fitting to the observed real data compared with the classical integer order models. Fractional order models take into consideration, the phenomenon of memory which exists in biological and epidemiological systems [21-28]. The constant fractional order can be considered as the index of the memory [29-34]. The fractional variable-order derivatives which are described as an extension of the constant fractional-order derivatives that can be used to characterize the memory that changes with time [35].
As shown in the literature, the numerical results of the fractional order models are more precise in several applications [36-38]. Motivated by this, in this study we present a fractional variable-order SISI model to describe the dynamics of MERS-CoV pandemic. The main contribution of this paper is to study the impact of the time-varying fractional derivative on the numerical results. Hence, we introduce several fractional variable-order derivatives to the proposed model in order to

* Corresponding author e-mail: mkibrahim@msa.edu.eg

show that, when the fractional derivatives vary with time, the behavior of the numerical solutions of the model dramatically changes.
The rest of the paper is organized as follows. Some basic definitions about the fractional variable-order derivatives are presented in section 2 while in section 3, the proposed fractional variable-order model of MERS-COV is introduced. Equilibrium points and stability are discussed in section 4. The Numerical results of the proposed model are presented and discussed in Section 5. The conclusion of the paper is given in section 6 to summarize and highlight the main points of our work.

2 Fractional calculus

In this section, some basic definitions of the fractional variable-order derivatives which are considered as a generalization of the constant fractional-order derivatives [38] are presented. The non-integer variable-order derivative can depict the variable memory of the fractional order models (FOM). Caputo derivative is commonly used in mathematical models because the initial conditions of the FOM are the same as the initial conditions of the classical integer-order models [38-40]. There exists different approaches to define the fractional variable-order derivatives. In the following definitions, the fractional variable-order $0 < \alpha(t) \leq 1$ is a continuous bounded function [40].

2.1

$$ {}^{GL}_{0}D_{t}^{\alpha(t)} g(t) = \lim_{h\to 0} h^{-\alpha} \sum_{i=0}^{[n]} (-1)^{i} \binom{\alpha}{i} g(t-ih) $$

2.2 Caputo derivatives:

2.2.1 Left Caputo derivative

$$ {}^{C}_{a}D_{t}^{\alpha(t)} g(t) = \frac{1}{\Gamma(1-\alpha(t))} \int_{a}^{t} (t-s)^{-\alpha(t)} g'(s)\, ds \tag{1} $$

2.2.2 Right Caputo derivative:

$$ {}^{C}_{t}D_{b}^{\alpha(t)} g(t) = \frac{-1}{\Gamma(1-\alpha(t))} \int_{t}^{b} (s-t)^{-\alpha(t)} g'(s)\, ds \tag{2} $$

2.3 R-L derivative:

2.3.1 Left R-L derivative:

$$ {}^{RL}_{a}D_{t}^{\alpha(t)} g(t) = \frac{1}{\Gamma(1-\alpha(t))} \frac{d}{dt} \int_{a}^{t} (t-s)^{-\alpha(t)} g(s)\, ds \tag{3} $$

2.3.2 Right R-L derivative:

$$ {}^{RL}_{b}D_{t}^{\alpha(t)} g(t) = \frac{-1}{\Gamma(1-\alpha(t))} \frac{d}{dt} \int_{t}^{b} (s-t)^{-\alpha(t)} g(s)\, ds \tag{4} $$

Caputo fractional variable-order derivative is used here in this paper as it can employ the same traditional initial conditions of the integer order derivative which are physically comprehensible.

3 Model derivation

In this section, a fractional variable-order model of MERS-COV will be implemented based on the model presented in [41,42]. The population is divided into two areas x and y in the presented model. There are two sub-populations in each area according to their disease status; the infected population (I_x and I_y) and the population who are susceptible to infection (S_x and S_y).
The Fractional variable-order model of MERS-CoV is as follows:

$$\begin{aligned}
D^{\alpha(t)}I_x(t) &= \frac{\beta S_x I_x}{S_x+I_x} - (c+d+\mu_1)I_x + \mu_2 I_y + \frac{\omega\mu_2 S_y I_y}{S_y+I_y},\\
D^{\alpha(t)}I_y(t) &= \frac{\beta S_y I_y}{S_y+I_y} - (c+d+\mu_2)I_y + \mu_1 I_x + \frac{\omega\mu_1 S_x I_x}{S_x+I_x},\\
D^{\alpha(t)}S_x(t) &= a_1 - \frac{\beta S_x I_x}{S_x+I_x} - (b+a_1)S_x + \mu_2 S_y + dI_x - \frac{\omega\mu_2 S_y I_y}{S_y+I_y},\\
D^{\alpha(t)}S_y(t) &= a_2 - \frac{\beta S_y I_y}{S_y+I_y} - (b+a_2)S_y + \mu_1 S_x + dI_y - \frac{\omega\mu_1 S_x I_x}{S_x+I_x}
\end{aligned} \tag{5}$$

With the same initial conditions $I_x(0)=100, I_y(0)=0, S_x(0)=500, S_y(0)=500$.

Where the variable order $\alpha(t)$ is a function of time and the parameters are described as follows:
- β is the transmission rate within an area
- ω is the transmission rate in different area
- b is the rate of natural death of the susceptible individuals
- c is the rate of MERS-CoV death of human population
- d is the rate of recovery from MERS-CoV
- a_1 is the number of persons added to S_x
- a_2 is the number of persons added to S_y
- μ_1 is the rate of movement from region x to region y
- μ_2 is the rate of movement from region y to region x

The Parameters of the presented system have been taken from [41,42] as follows:

$$a_1 = 4326, a_2 = 13461, b = 0.01, c = 0.05, d = 0.1, \beta = 0.1, \omega = 1, \mu_2 = 0.$$

The value of the parameter μ_1 varies. The given system will be solved in two cases. In the 1^{st} case, $\mu_1 = 0.1$ while in the 2^{nd} case $\mu_1 = 0.01$. The same initial conditions which have been taken from [41.42] will be used in the two cases as follows:

$$I_x(0) = 100, I_y(0) = 0, S_x(0) = 500, S_y(0) = 500.$$

4 Equilibrium points and stability

The proposed model (5) can be written as follows:

$$\begin{aligned}
D^{\alpha(t)}I_x(t) &= f_1(I_x, I_y, S_x, S_y),\\
D^{\alpha(t)}I_y(t) &= f_2(I_x, I_y, S_x, S_y),\\
D^{\alpha(t)}S_x(t) &= f_3(I_x, I_y, S_x, S_y),\\
D^{\alpha(t)}S_y(t) &= f_4(I_x, I_y, S_x, S_y)
\end{aligned} \tag{6}$$

Where $I_x(0) = I_{x0}, I_y(0) = I_{y0}, S_x(0) = S_{x0}$, and $S_y(0) = S_{y0}$

To get the equilibrium points of the fractional variable-order system (5),

$$\begin{aligned} \text{let} \quad & D^{\alpha(t)}(I_x) = D^{\alpha(t)}(I_y) = D^{\alpha(t)}(S_x) = D^{\alpha(t)}(S_y) = 0 \\ & \Rightarrow f_i\left(I_{x_{eq}}, I_{y_{eq}}, S_{x_{eq}}, S_{y_{eq}}\right) = 0, i = 1,2,3,4. \end{aligned}$$

The presented model (5) has two equilibrium points, the free equilibrium point E_0 and the endemic equilibrium point E_1. The free equilibrium point E_0 outlines the circumstances where I_x and I_y do not exist. On the other hand, the endemic equilibrium point E_1 portrays the situation where all the population groups S_x, S_y, I_x and I_y exist.

The disease free equilibrium point $E_0 = \left(0,0,\frac{a_2\mu_2+a_1(b+\mu_2)}{b(\mu_1+\mu_2+b)},\frac{a_1\mu_1+a_2(b+\mu_1)}{b(\mu_1+\mu_2+b)}\right)$ and the endemic equilibrium point $E_1 = (I_x^*, I_y^*, S_x^*, S_y^*)$. The local stability of $\left(I_{x_{eq}}, I_{y_{eq}}, S_{x_{eq}}, S_{y_{eq}}\right)$ is satisfied under condition that, the Jacobian's eigenvalues J satisfy the following condition [9]:

$$|arg(\sigma_i)| > \frac{\alpha(t)\pi}{2}$$

Where

$$J = \begin{bmatrix} \frac{\partial f_1}{\partial I_x} & \frac{\partial f_1}{\partial I_y} & \frac{\partial f_1}{\partial S_x} & \frac{\partial f_1}{\partial S_y} \\ \frac{\partial f_2}{\partial I_x} & \frac{\partial f_2}{\partial I_y} & \frac{\partial f_2}{\partial S_x} & \frac{\partial f_2}{\partial S_y} \\ \frac{\partial f_3}{\partial I_x} & \frac{\partial f_3}{\partial I_y} & \frac{\partial f_3}{\partial S_x} & \frac{\partial f_3}{\partial S_y} \\ \frac{\partial f_4}{\partial I_x} & \frac{\partial f_4}{\partial I_y} & \frac{\partial f_4}{\partial S_x} & \frac{\partial f_4}{\partial S_y} \end{bmatrix}$$

For the free equilibrium point, the eigenvalues are

$$\begin{aligned} \sigma_1 &= -b < 0, \\ \sigma_2 &= -(b+\mu_1+\mu_2), \\ \sigma_3 &= (2\beta - 2c - 2d - \mu_1 - \mu_2 + \sqrt{\xi})/2, \\ \sigma_4 &= (2\beta - 2c - 2d - \mu_1 - \mu_2 - \sqrt{\xi})/2, \\ \xi &= \mu_1^2 + 2(1+4\omega+2\omega^2)\mu_1\mu_2 + \mu_1^2 > 0. \end{aligned}$$

The free equilibrium point E_0 is locally asymptotically stable if $\sigma_{3,4} < 0$, but for the sufficient condition of the endemic equilibrium point E_1 to be locally asymptotically stable is:

$$|arg(\sigma_1)| > \frac{\alpha(t)\pi}{2}, |arg(\sigma_2)| > \frac{\alpha(t)\pi}{2}, |arg(\sigma_3)| > \frac{\alpha(t)\pi}{2}, |arg(\sigma_4)| > \frac{\alpha(t)\pi}{2}$$

The negative eigenvalues which appear in several applications like epidemiology, hydrostatic fluid and buckling analyses applications mean that, the solutions of the dynamical system decay with time [44]. Such eigenvalues can be used to predict if the pandemic eventually dies out or not as the largest eigenvalue represents the basic reproduction number R_0 in order to control the spread of infectious diseases [45]. For model (5), R_0 is given as:

$$R_0 = \frac{\beta(\mu_1+\mu_2+2c+2d) + 2\mu_1\mu_2\omega + \sqrt{\eta}}{2(\mu_1+\mu_2)(c+d) + (c+d)^2} \tag{7}$$

Where

$$\eta = \beta^2(\mu_1+\mu_2)^2 + 4\mu_1\mu_2\omega((c+d+\mu_2)(c+d+\mu_1)\omega + 2\beta(\frac{1}{2}\mu_1 + \frac{1}{2}\mu_2 + c + d))$$

Theorem 1 [43]
E_0 is locally asymptomatically stable if $R_0 < 1$, where as E_0 is unstable if $R_0 > 1$.
Theorem 2 [43]
The disease-free equilibrium E_0 is globally asymptotically stable if $R_0 < 1$.
If $R_0 < 1$,then the outbreak is expected to end but if $R_0 > 1$, then the outbreak is expected to persist. This explains the connection between the existence or stability of the endemic point E_1 and the value of R_0.

5 Numerical results

We use the predictor-corrector scheme to find the numerical solutions of the presented model (5). However, the predictor-corrector technique uses the average of the slopes of the tangent to the solution curve over an interval rather than a single point in order to decrease the error [46-48].
Consequently, for system (6), suppose a uniform grid $\{t_j = jh : j = 0,1,...,n\}$, where n is an integer such that $n = T/h, 0 < \alpha(t) \leq 1, 0 \leq t \leq T$, and $T \in \mathbb{R}^+$.
The predictor approximations are presented as follows:

$$\begin{aligned}
(I_x)^p_{n+1} &= I_x(0) + \frac{1}{\Gamma(\alpha(t_{n+1}))} \sum_{j=0}^{n} B_{j,n+1} f_1\left(t_j, (I_x)_j, (I_y)_j, (S_x)_j, (S_y)_j\right), \\
(I_y)^p_{n+1} &= I_y(0) + \frac{1}{\Gamma(\alpha(t_{n+1}))} \sum_{j=0}^{n} B_{j,n+1} f_2\left(t_j, (I_x)_j, (I_y)_j, (S_x)_j, (S_y)_j\right), \\
(S_x)^p_{n+1} &= S_x(0) + \frac{1}{\Gamma(\alpha(t_{n+1}))} \sum_{j=0}^{n} B_{j,n+1} f_3\left(t_j, (I_x)_j, (I_y)_j, (S_x)_j, (S_y)_j\right), \\
(S_y)^p_{n+1} &= S_y(0) + \frac{1}{\Gamma(\alpha(t_{n+1}))} \sum_{j=0}^{n} B_{j,n+1} f_4\left(t_j, (I_x)_j, (I_y)_j, (S_x)_j, (S_y)_j\right),
\end{aligned} \tag{8}$$

Where

$$B_{j,n+1} = \frac{h^{\alpha(t_{n+1})}}{\alpha(t_{n+1})}[(n-j+1)^{\alpha(t_{n+1})} - (n-j)^{\alpha(t_{n+1})}], 0 \leq j \leq n.$$

The corrector approximation $(I_x)_{n+1}, (I_y)_{n+1}, (S_x)_{n+1}$ and $(S_y)_{n+1}$ are given by as follows:

$$\begin{aligned}
(I_x)_{n+1} &= I_x(0) + \frac{h^{\alpha(t_{n+1})}}{\Gamma(\alpha(t_{n+1})+2)} f_1(t_{n+1}, (I_x)^p_{n+1}, (I_y)^p_{n+1}, (S_x)^p_{n+1}, (S_y)^p_{n+1}) \\
&\quad + \frac{h^{\alpha(t_{n+1})}}{\Gamma(\alpha(t_{n+1})+2)} \sum_{j=0}^{n} A_{j,n+1} f_1(t_j, (I_x)_j, (I_y)_j, (S_x)_j, (S_y)_j). \\
(I_y)_{n+1} &= I_y(0) + \frac{h^{\alpha(t_{n+1})}}{\Gamma(\alpha(t_{n+1})+2)} f_2(t_{n+1}, (I_x)^p_{n+1}, (I_y)^p_{n+1}, (S_x)^p_{n+1}, (S_y)^p_{n+1}) \\
&\quad + \frac{h^{\alpha(t_{n+1})}}{\Gamma(\alpha(t_{n+1})+2)} \sum_{j=0}^{n} A_{j,n+1} f_2(t_j, (I_x)_j, (I_y)_j, (S_x)_j, (S_y)_j). \\
(S_x)_{n+1} &= S_x(0) + \frac{h^{\alpha(t_{n+1})}}{\Gamma(\alpha(t_{n+1})+2)} f_3(t_{n+1}, (I_x)^p_{n+1}, (I_y)^p_{n+1}, (S_x)^p_{n+1}, (S_y)^p_{n+1}) \\
&\quad + \frac{h^{\alpha(t_{n+1})}}{\Gamma(\alpha(t_{n+1})+2)} \sum_{j=0}^{n} A_{j,n+1} f_3(t_j, (I_x)_j, (I_y)_j, (S_x)_j, (S_y)_j). \\
(S_y)_{n+1} &= S_y(0) + \frac{h^{\alpha(t_{n+1})}}{\Gamma(\alpha(t_{n+1})+2)} f_4(t_{n+1}, (I_x)^p_{n+1}, (I_y)^p_{n+1}, (S_x)^p_{n+1}, (S_y)^p_{n+1}) \\
&\quad + \frac{h^{\alpha(t_{n+1})}}{\Gamma(\alpha(t_{n+1})+2)} \sum_{j=0}^{n} A_{j,n+1} f_4(t_j, (I_x)_j, (I_y)_j, (S_x)_j, (S_y)_j).
\end{aligned} \tag{9}$$

Where

$$A_{j,n+1} = \begin{cases} n^{\alpha(t_{n+1})+1} - [n - \alpha(t_{n+1})](n+1)^{\alpha(t_{n+1})} & j = 0 \\ (n-j+2)^{\alpha(t_{n+1})+1} - 2(n-j+2)^{\alpha(t_{n+1})+1} + (n-j)^{\alpha(t_{n+1})+1} & 1 \leq j \leq n \\ 1 & j = n+1 \end{cases} \tag{10}$$

The presented model has been solved by predictor-corrector method for different values of $\alpha(t)$. The predictor-corrector numerical results have been compared with the numerical results of the classical fourth order Runge-Kutta method (RK4) at $\alpha(t) = 1$ in order to check the accuracy of the predictor-corrector method. As shown in figure 1, the results of the two methods are very close to each other.

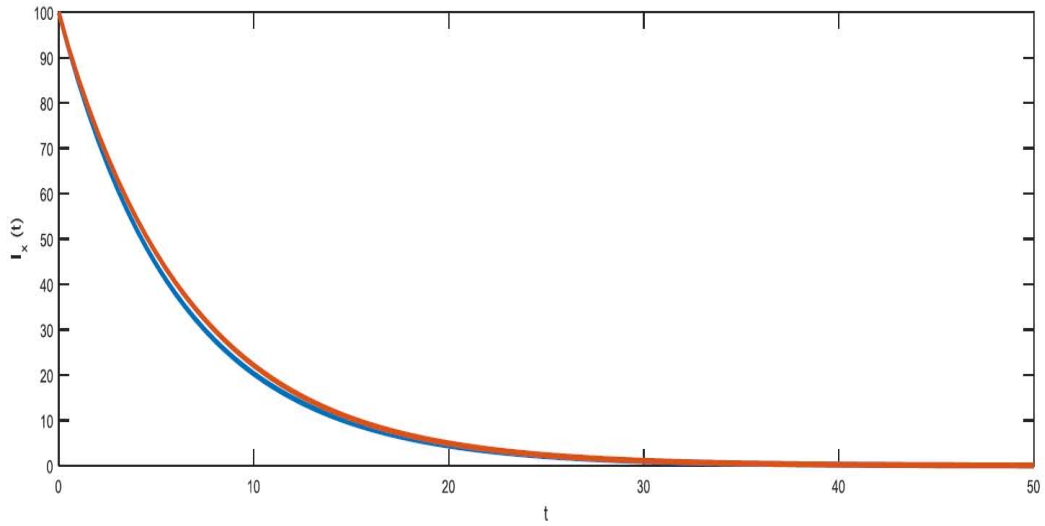

Fig. 1: The infected population I_x at $\alpha(t) = 1$ using the predictor-corrector method (the red line)and the RK4 method (the blue line)

.

When $\mu_1 = 0.1$, the basic reproduction number $R_0 < 1$ and the disease free equilibrium point E_0 is asymptotic stable (see figures. 2-7), while $R_0 > 1$ and the endemic equilibrium point E_1 is asymptotic stable when $\mu_1 = 0.01$ (see figures. 8-13). The fractional-order derivative considers the memory effects of the system, while the variable fractional-order shows that the memory effect of proposed model dramatically changes with time. The behavior of the system is investigated for different values of $\alpha(t)$. When $\alpha(t) = 1 - 0,01t$ and $\alpha(t) = 0.75 - 0.01/10t$ which are decreasing functions at which the memory is decreasing. Hence, the behaviour of the numerical solution is slower with time as shown in figures (2, 4, 5, 7, 8, 10, 11, 13). On the other hand, when $\alpha(t)$ is considered as a periodic, then the memory is periodic. In addition, the behavior of the numerical solution is periodic. as in the presented figures (3, 6, 9, 12) where $\alpha(t) = 0.7 - 0.01sin(\pi t)$.

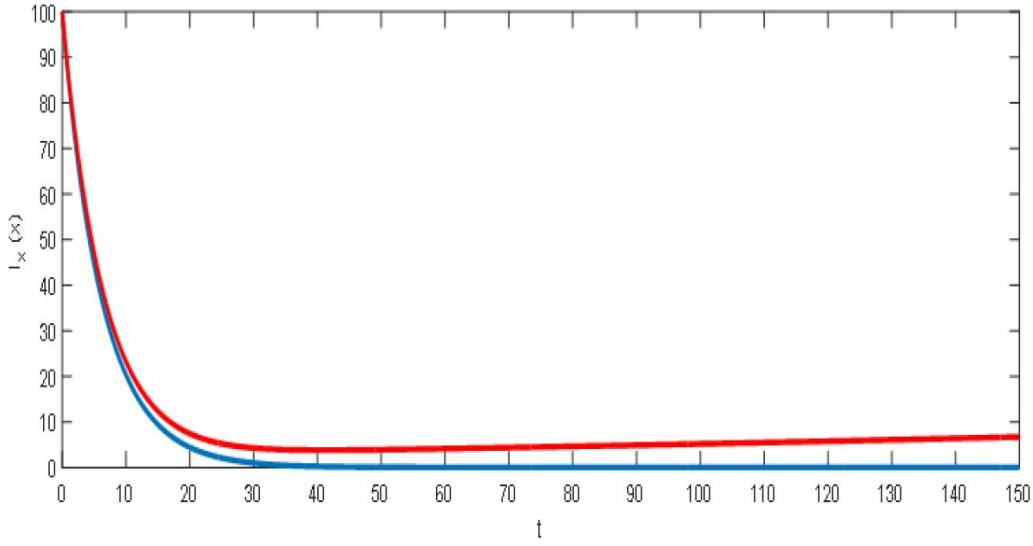

Fig. 2: The infected population I_x when $\mu_1 = 0.1$: blue line $(\alpha(t) = 1)$, red line $(\alpha(t) = 1 - 0.01t)$.

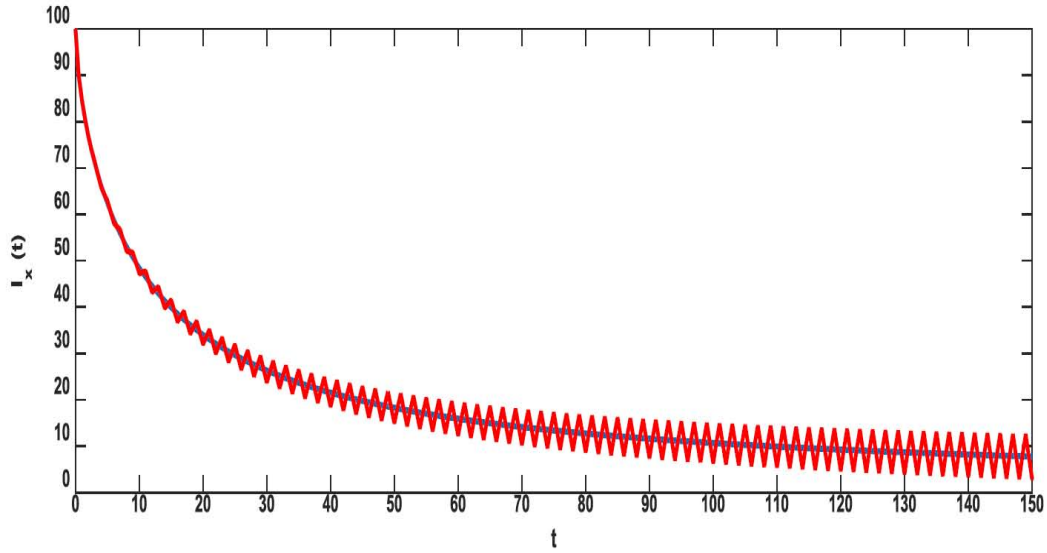

Fig. 3: The infected population I_x when $\mu_1 = 0.1$: blue line $(\alpha(t) = 0.7)$, red line $(\alpha(t) = 0.7 - 0.01\sin(\pi t))$.

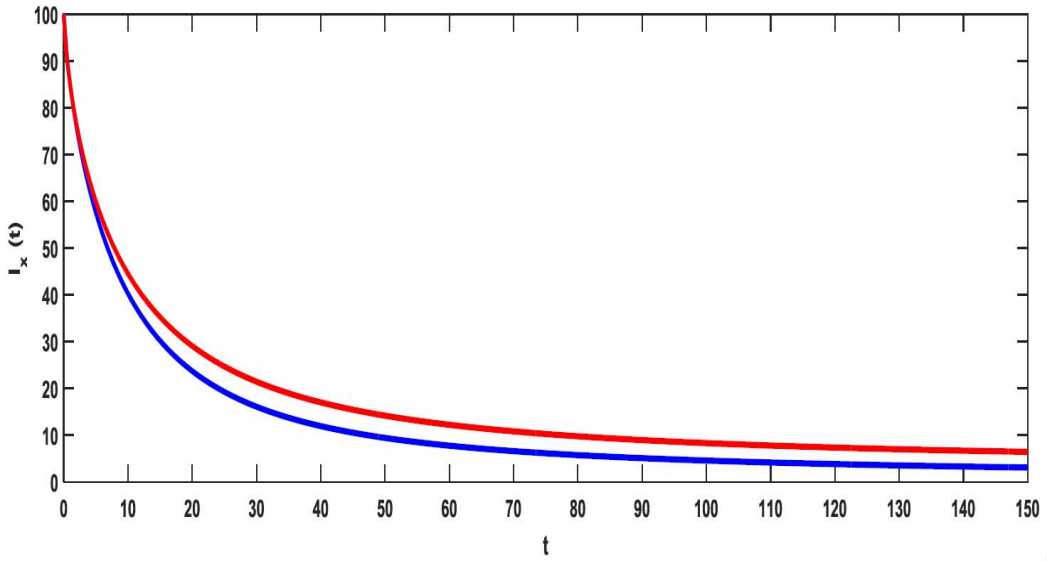

Fig. 4: The infected population I_x when $\mu_1 = 0.1$: blue line $(\alpha(t) = 0.8)$, red line $(\alpha(t) = 0.75 - \frac{0.01}{100}t)$.

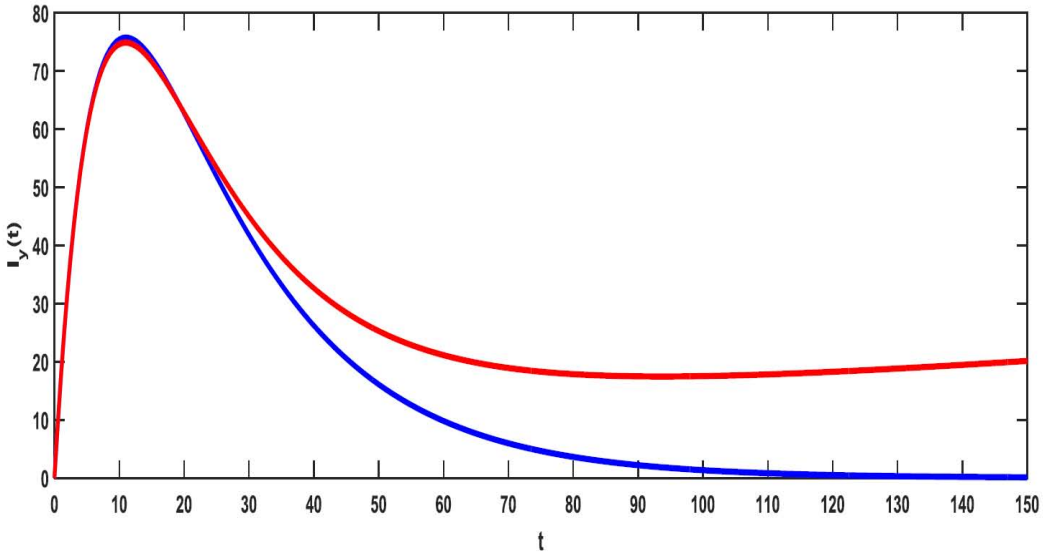

Fig. 5: The infected population I_y when $\mu_1 = 0.1$: blue line $(\alpha(t) = 1)$, red line $(\alpha(t) = 1 - 0.01t)$.

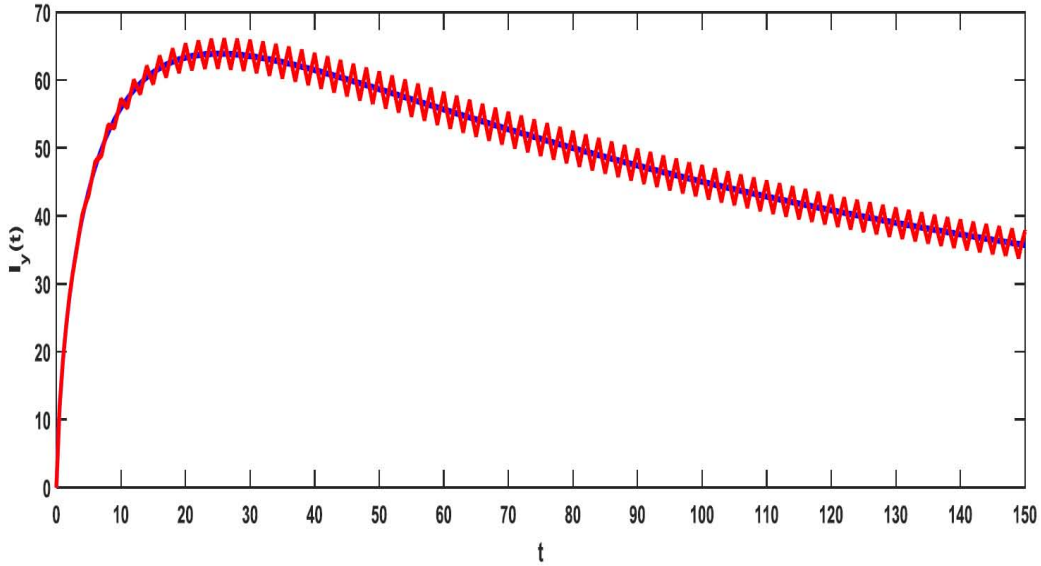

Fig. 6: The infected population I_y when $\mu_1 = 0.1$: blue line $(\alpha(t) = 0.7)$, red line $(\alpha(t) = 0.7 - 0.01\sin(\pi t))$.

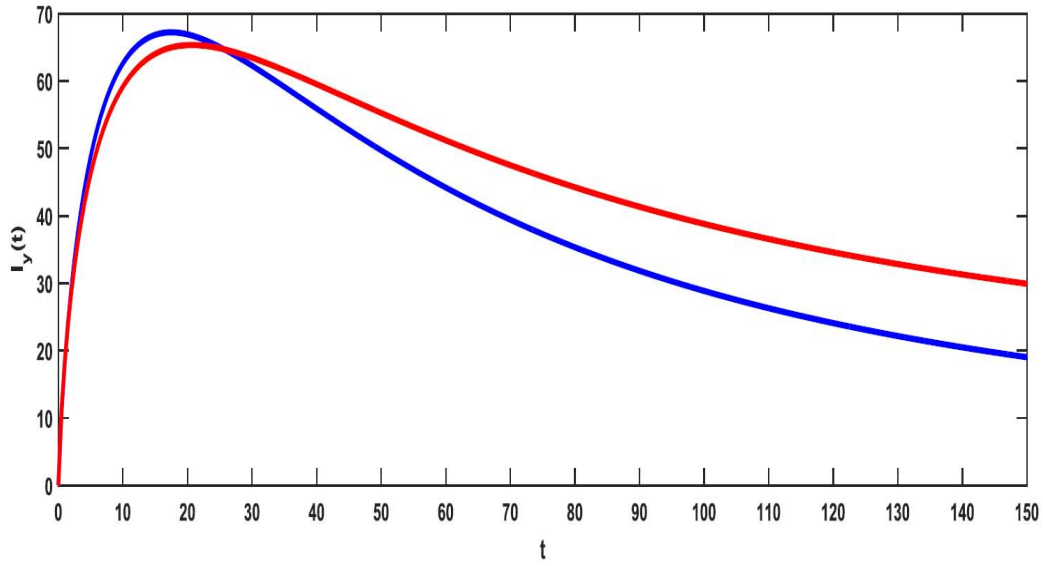

Fig. 7: The infected population I_x when $\mu_1 = 0.1$: blue line $(\alpha(t) = 0.8)$, red line $(\alpha(t) = 0.75 - \frac{0.01}{100}t)$.

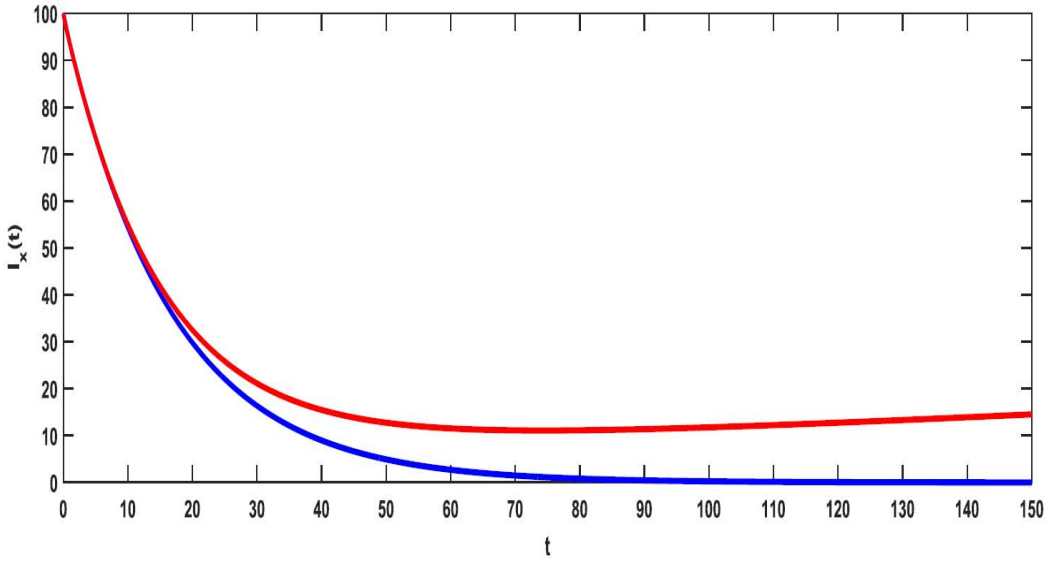

Fig. 8: The infected population I_x when $\mu_1 = 0.01$: blue line $(\alpha(t) = 1)$, red line $(\alpha(t) = 1 - 0.01t)$.

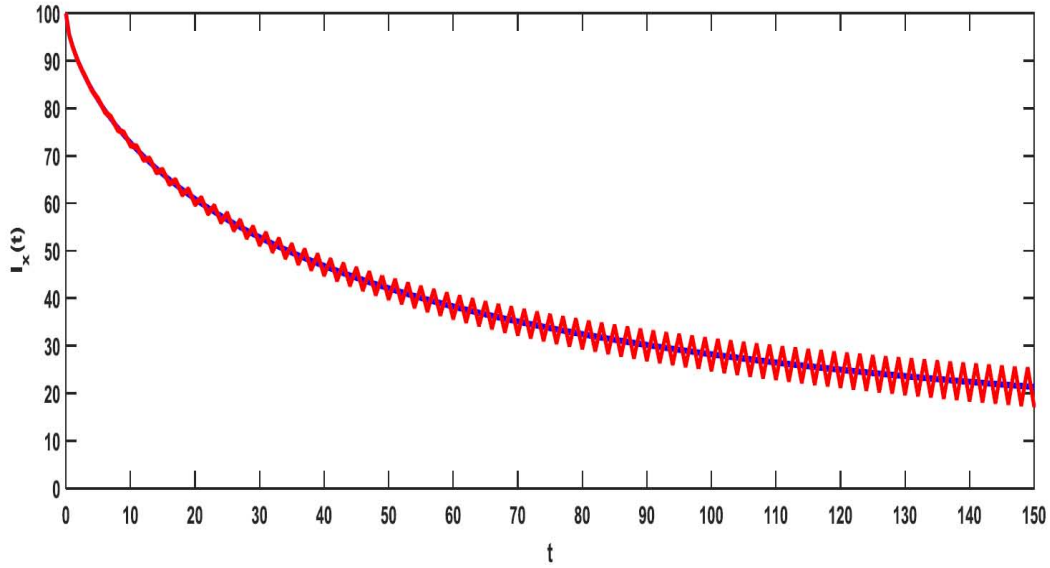

Fig. 9: The infected population I_x when $\mu_1 = 0.01$: blue line $(\alpha(t) = 0.7)$, red line $(\alpha(t) = 0.7 - 0.01\sin(\pi t))$.

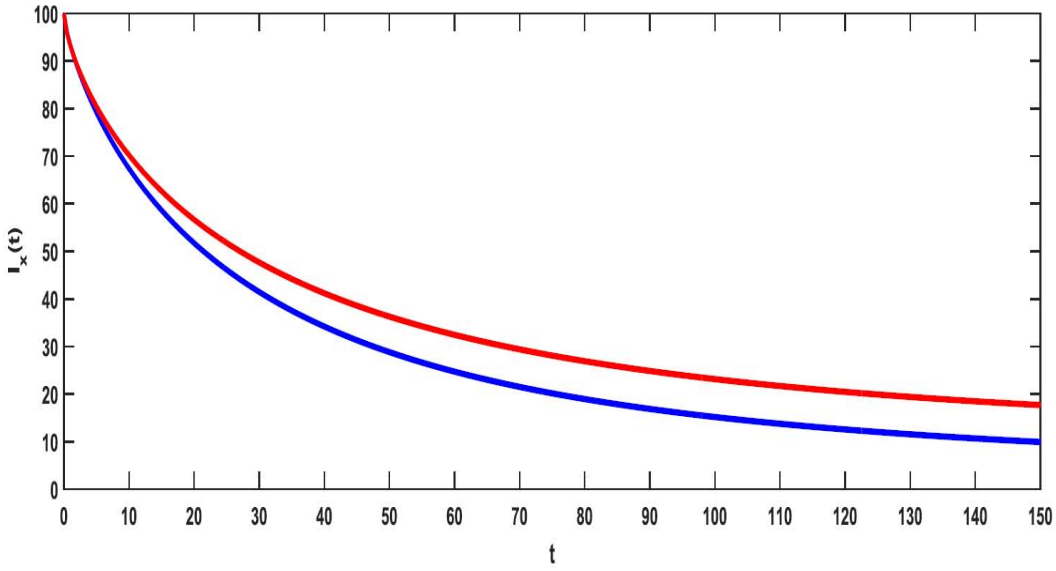

Fig. 10: The infected population I_x when $\mu_1 = 0.01$: blue line $(\alpha(t) = 0.8)$, red line $(\alpha(t) = 0.75 - \frac{0.01}{100}t)$.

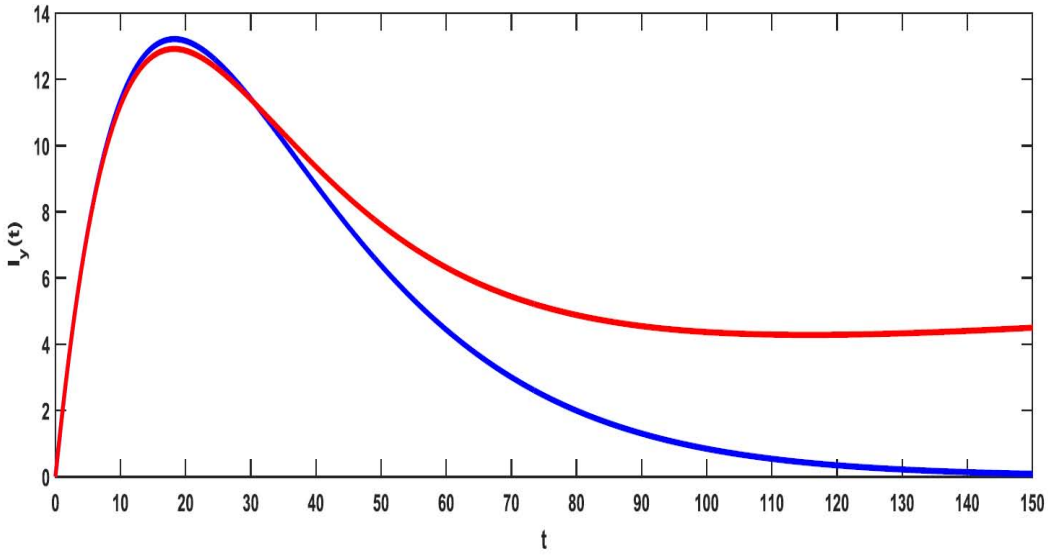

Fig. 11: The infected population I_y when $\mu_1 = 0.01$: blue line $(\alpha(t) = 1)$, red line $(\alpha(t) = 1 - 0.01t)$.

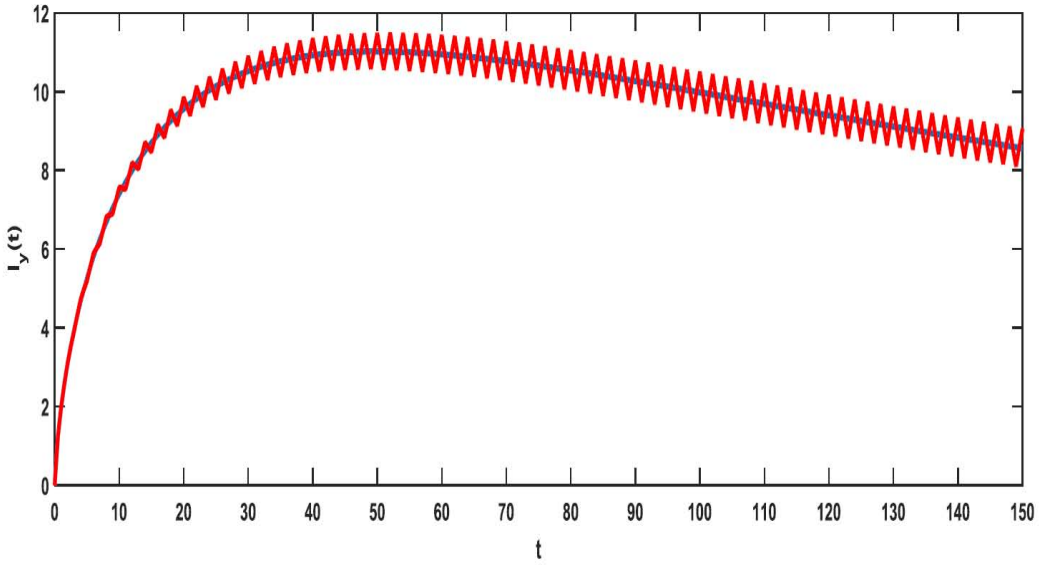

Fig. 12: The infected population I_y when $\mu_1 = 0.01$: blue line $(\alpha(t) = 0.7)$, red line $(\alpha(t) = 0.7 - 0.01\sin(\pi t))$

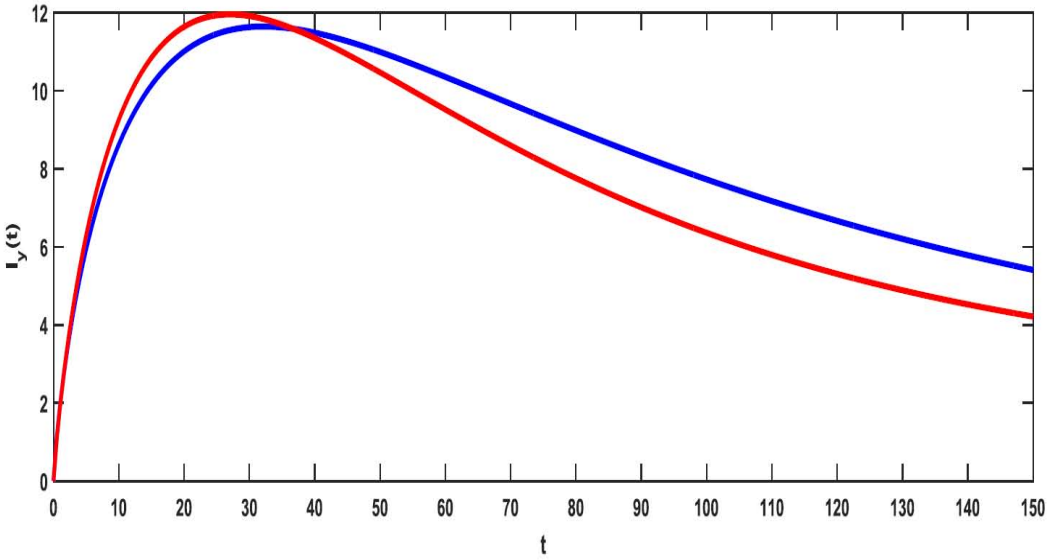

Fig. 13: The infected population I_y when $\mu_1 = 0.01$: blue line $(\alpha(t) = 0.9)$, red line $(\alpha(t) = 0.75 - \frac{0.01}{100}t)$

6 Conclusion

We argue that, using the proposed fractional variable-order models offers a well understanding of the dynamics of the of MERs-CoV pandemic. The impact of introducing time-varying fractional derivatives on the numerical solutions has been discussed. This study indicates that, the non-integer variable-order models have the advantage of distinguishing the long memory that changes with time. So, the fractional variable-order derivative can be employed to depict the variable memory of systems. The predictor-corrector approach is used to solve the proposed MERs-CoV model. Furthermore, the stability analysis of the system has been illustrated.

References

[1] M.M. Khader and M. Adel, Modeling and numerical simulation for covering the fractional COVID-19 model using spectral collocation-optimization algorithm, *Fractal Fract.* **6**(7), 363 (2022).
[2] T. Burki, Understanding the history of infectious diseases, *Lancet Infect. Dis.* **22**(5), 602 (2022).
[3] M. Khalil, A game theory-based fractional order model for the simulation of human responses in an emerging epidemic, *Progr. Fract. Differ. Appl.* **8**(3), 447-457 (2022).
[4] A. M. A. El-Sayed, A. A. M. Arafa, I. M. Hanafy and M. I. Gouda, A fractional-order model of dengue fever with awareness effect, numerical solutions and asymptotic stability analysis, *Progr. Fract. Differ. Appl.* **8**(2), 267-274 (2022).
[5] N. H. Sweilam, W. A. Kareem, S. Al-Mekhlafi and Z. Nabih, Numerical treatments for a complex order fractional HIV infection model with drug resistance during therapy, *Progr. Fract. Differ. Appl.* **7**(3), 163-176 (2021).
[6] M. J. Keeling and P. Rohani, *Modeling infectious diseases in humans and animals*, Princeton Univ. Press, 2008.
[7] World Health Organization, Middle East respiratory syndrome coronavirus (MERS-CoV), summary of current situation, literature update and risk assessment (2015).
[8] Z. A. Memish, S. Perlman, M. D. V. Kerkhove and A. Zumla, Middle East respiratory syndrome, *Lancet* **395**(10229), 1063-1077 (2020).
[9] R. F Ceylan and B. Ozkan, The economic effects of epidemics: from SARS and MERS to COVID-19, *J. Adv. Soc. Sci. Humanit.* **1**(2), 21-29 (2020).
[10] A. A. M. Arafa, S. Z. Rida and M. Khalil, Fractional modeling dynamics of HIV and CD4+ Tcells during primary infection, *Nonlin. Biomed. Phys.* **6**(1), 1-7 (2012).
[11] A. A. M. Arafa, S. Z. Rida and M. Khalil, A fractional-order model of HIV infection: numerical solution and comparisons with data of patients, *Int. J. Biomath.* **7**(04), (2014).
[12] A. A. M. Arafa, S. Z. Rida and M. Khalil, The effect of anti-viral drug treatment of human immunodeficiency virus type 1 (HIV-1) described by a fractional order model, *Appl. Math. Mod.* **37**(4), 2189-2196 (2013).

[13] A. A. M Arafa, S. Z. Rida, and M. Khalil, A fractional-order model of HIV infection with drug therapy effect, *J. Egypt. Math. Soc.* **22**(3), 538-543 (2014).
[14] A. M. A El-Sayed, A. A. M Arafa, M. Khalil, A. Sayed, Backward bifurcation in a fractional order epidemiological model, *Progr. Fract. Differ. Appl.* **3**(4), 1-8 (2017).
[15] Y. Ibrahim, M. M. Khader, A. Megahed , A. El-Salam and M. Adel, An efficient numerical simulation for the fractional COVID-19 model using the GRK4M together with the fractional FDM, *Fractal Fract.* **6**(6), 304 (2022).
[16] N. H. Sweilam, A. M. Nagy and L. E. Elfahri, Fractional-order delayed Salmonella transmission model: a numerical simulation, *Progr. Fract. Differ. Appl.* **8**(1), 63-76 (2022).
[17] N. H. Sweilam and M. M. Abou Hasan, Efficient method for fractional Levy-Feller advection dispersion equation using Jacobi polynomials, *Progr. Fract. Differ. Appl.* **6**(2), 115-128 (2020).
[18] N. H. Sweilam, F. A. Rihan and S. M. Al-Mekhlafi, A fractional-order delay differential model with optimal control for cancer treatment based on synergy between anti-angiogenic and immune cell therapies, *Disc. Contin. Dyn. Sys. Ser. S* **13**(9), 2403 (2020).
[19] F. A. Rihan and V. Gandhi, Dynamics and sensitivity of fractional-order delay differential model for coronavirus (COVID-19) infection, *Progr. Fract. Differ. Appl.* **7**(1), 43-61 (2021).
[20] A. V. Chechkin, V. Y. Gonchar, R. Gorenflo, N. Korabel and I. M. Sokolov, Generalized fractional diffusion equations for accelerating sub diffusion and truncated Lévy flights, *Phys. Rev. E* **78**(2), 021111 (2008).
[21] A. V. Chechkin, R. Gorenflo and I. M. Sokolov, Fractional diffusion in inhomogeneous media, *J. Phys. A: Math. Gen.* **38**(42), L679 (2005).
[22] K. Diethelm, *The analysis of fractional differential equations. An application-oriented exposition using differential operators of Caputo type*, *Lect. Notes Math.*, Vol. 2004, Springer, 2010.
[23] C. Li and W. Deng, Remarks on fractional derivatives, *Appl. Math. Comput.* **187**(2), 777-784 (2007).
[24] D. Matignon, Stability results for fractional differential equations with applications to control processing. In computational engineering in systems applications, Lille, France: IMACS, IEEESMC. 2, 963-968, 1996.
[25] C. A. Monje, Y. Q. Chen, B. M. Vinagre, D. Xue and V. Feliu-Batlle, *Fractional-order systems and controls: fundamentals and applications*, Springer Science & Business Media, 2010.
[26] I. Podlubny, An introduction to fractional derivatives, fractional differential equations, to methods of their solution and some of their applications, *Math. Sci. Eng.* **198**, (1998).
[27] S. G. Samko, Fractional integration and differentiation of variable order, *Anal. Math.* **21**(3), 213-236 (1995).
[28] S. G. Samko and B. Ross, Integration and differentiation to a variable fractional order, *Integr. Transf. Spec. Func.* **1**(4), 277-300 (1993).
[29] W. Smit and H. De Vries, Rheological models containing fractional derivatives, *Rheol. Acta* **9**(4), 525-534 (1970).
[30] E. Ahmed, A. M. A. El-Sayed and H. A. El-Saka, Equilibrium points, stability and numerical solutions of fractional-order predator–prey and rabies models, *J. Math. Anal. Appl.* **325**(1), 542-553 (2007).
[31] H. A. El-Saka, P. Ahmed, M. I. Shehata and A. M. A. El-Sayed, On stability, persistence, and Hopf bifurcation in fractional order dynamical systems, *Nonlin. Dyn.* **56**(1-2), 121 (2009).
[32] Y. Li, Y. Chen and I. Podlubny, Stability of fractional-order nonlinear dynamic systems: Lyapunov direct method and generalized Mittag–Leffler stability, *Comput. Math. Appl.* **59**(5), 1810-1821 (2010).
[33] A. M. A El-Sayed, A. A. M Arafa, M. Khalil and A. Sayed, Backward bifurcation in a fractional order epidemiological model, *Progr. Fract. Differ. Appl.* **3**(4), 281-287 (2017).
[34] M. El-Kady and A. El-Sayed, Fractional differentiation matrices for solving fractional orders differential equations, *Int, J. Pure Appl. Math.* **84**(2), 1-13 (2013).
[35] A. Atangana and A. H. Cloot, Stability and convergence of the space fractional variable-order Schrödinger equation, *Adv. Differ. Equ.* **1**, 1-10 (2013).
[36] A. H. Bhrawy and M. A. Zaky, Numerical simulation for two-dimensional variable-order fractional nonlinear cable equation, *Nonlin. Dyn.* **80**(1), 101-116 (2015).
[37] N.H. Sweilam and S.M. AL-Mekhlafi, Numerical study for multi-strain tuberculosis (TB) model of variable-order fractional derivatives, *J. Adv. Res.* **7**(2), 271-283 (2016).
[38] Y. Xu and Z. He, Existence and uniqueness results for Cauchy problem of variable-order fractional differential equations, *J. Appl. Math. Comput.* **43**(1-2), 295-306 (2013).
[39] C.F. Lorenzo and T.T. Hartley, Variable order and distributed order fractional operators, *Nonlin. Dyn.* **29**(1-4), 57-98 (2002).
[40] A.A.M. Arafa, M. Khalil and A. Sayed, A non-integer variable order mathematical model of human immunodeficiency virus and malaria coinfection with time delay, *Complexity* **1**, 1-13 (2019).
[41] B. Yong and L. Owen, Dynamical transmission model of MERS-CoV in two areas, *AIP Conference Proceedings* **1716**(1), 020010 (2016).
[42] E. Ahmed and H.A.EL-Saka, On a fractional orders study of Middle East respiratory syndrome corona virus (MERS-COV), *J. Frac. Cal. App.* **8**(1), 118-126 (2017).
[43] J. Jia and J. Xiao, Stability analysis of a disease resistance SEIRS model with nonlinear incidence rate, *Adv. Differ. Equ.* (1), 1-13 (2018).
[44] H.J. Ricardo, A modern introduction to differential equations, Academic Press, 2020.
[45] A.K. Supriatna, N. Anggriani, E. Carnia and A. Raihan, Eigen values in epidemic and other bioinspired models, *AIP Conference Proceedings* **1868**(1), 2017.

[46] K. Diethelm, N.J. Ford and A.D. Freed, A predictor-corrector approach for the numerical solution of fractional differential equations, *Nonlin. Dyn.* **29**, 3-22 (2002).
[47] M. Khalil, A.A.M. Arafa and A. Sayed, A variable fractional order network model of zika virus, *J. Fract. Calc. Appl.* **9**(1), 204–221 (2018).
[48] N.H. Sweilam, M. Khalil and A. Sayed, A fractional variable order model of COVID-19 Pandemic, *Progr. Fract. Differ. Appl.* **8**(4), 475-484 (2022).